Kinematic Signatures of Impulsive Supernova Feedback in Dwarf Galaxies

Jan D. Burger, Jesús Zavala, Laura V. Sales, Mark Vogelsberger, Federico Marinacci, and Paul Torrey

Kinematic signatures of impulsive supernova feedback in dwarf galaxies

Jan D. Burger*

Department of Physics and Astronomy, University of California, Riverside, CA, 92521, USA and
University of Iceland, Dunhagi 5, 107 Reykjavík, Iceland

Jesús Zavala

University of Iceland, Dunhagi 5, 107 Reykjavík, Iceland

Laura V. Sales

Department of Physics and Astronomy, University of California, Riverside, CA, 92521, USA

Mark Vogelsberger

MIT Kavli Institute for Astrophysics and Space Research, Ronald McNair Building, 37-611

Federico Marinacci

Department of Physics and Astronomy "Augusto Righi", University of Bologna, Bologna, I-40129, Italy

Paul Torrey

Department of Astronomy, University of Florida,
211 Bryant Space Sciences Center, Gainesville, FL 32611, USA

(Dated: September 16, 2022)

Impulsive supernova feedback and non-standard dark matter models, such as self-interacting dark matter (SIDM), are the two main contenders for the role of the dominant core formation mechanism at the dwarf galaxy scale. Here we show that the impulsive supernova cycles that follow episodes of bursty star formation leave distinct features in the distribution function of stars: groups of stars with similar ages and metallicities develop overdense shells in phase space. If cores are formed through supernova feedback, we predict the presence of such features in star-forming dwarf galaxies with cored host halos. **Their systematic absence would favor alternative dark matter models, such as SIDM, as the dominant core formation mechanism.**

I Introduction. One of the most persevering small-scale challenges [1] to the collisionless cold dark matter (CDM) paradigm concerns the inner density profiles of DM halos that host dwarf galaxies. Hints for constant density cores **observed in some dwarf galaxies** [2–7] appear to be at odds with the ubiquitous cusps predicted by CDM N-body simulations [8, 9]. To reconcile the success of the CDM paradigm at predicting the properties of the large-scale structure of the Universe with these observations on the scale of low-mass galaxies, a physical mechanism is required to remove the central DM cusps predicted by CDM N-body simulations [8, 9]. A potential way to flatten the central density profile of halos is through strong and impulsive fluctuations in the gravitational potential caused by supernova-driven episodes of gas removal [10–16]. For SNF to be effective, supernovae must occur in quasi-periodic cycles **and cause strong fluctuations in the central potential** on timescales that are shorter than the typical dynamical time in the galaxy, i.e., impulsively [11]. **As the time between the birth of a heavy ($\gtrsim 8\mathrm{M}_\odot$) star and its type II supernova explosion is less than ~ 40 Myrs, such quasi-periodic SN cycles can only be realized in** **galaxies with a bursty star formation history, i.e. a star formation rate that shows order of magnitude fluctuations over less than a dynamical time (see also [17]).** Although there is evidence of bursty star formation in dwarf galaxies at the high mass end [18], the duration of star bursts in the intermediate and low mass regime is far more uncertain [19, 20]. In cosmological simulations, SNF is most efficient at forming cores on the scale of bright dwarfs [12–14], **as long as the simulated star formation history is bursty and the gas dominates the binding energy in the inner halo before being expelled by feedback, causing a strong fluctuation in the total potential [15, 17].**

In modern sub-resolution models of the interstellar medium (e.g.[21, 22]), both the (average) burstiness of star formation and the maximal densities to which gas cools before forming stars can be regulated via a single numerical parameter set at the resolved scales in the simulations, the so-called SF threshold n_{th}, which gives the minimum density that gas needs to reach before it is eligible to form stars [15]. **In an otherwise fixed, idealized (non-cosmological) setup,** adopting larger values of n_{th} results in burstier SF**, more substantial potential fluctuations,** and thus more impulsive SNF, until eventually a threshold for core formation is reached **(see [16] for a discus-**
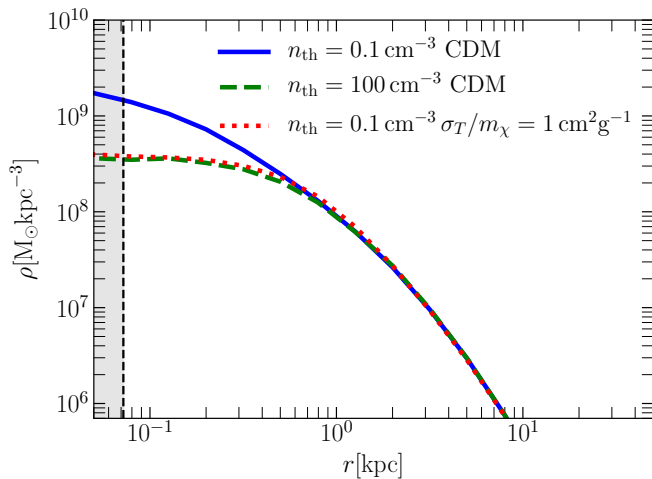
* jburger@ucr.edu

FIG. 1. Adiabatic and impulsive cusp-core transformation: Spherically averaged radial DM density of three different simulated dwarf-size halos after $3\,\mathrm{Gyr}$ of simulation time. The solid blue line corresponds to the CDM simulation with smooth star formation ($n_{\mathrm{th}} = 0.1\,\mathrm{cm}^{-3}$), whereas the dashed green line denotes the result of the CDM simulation with bursty star formation ($n_{\mathrm{th}} = 100\,\mathrm{cm}^{-3}$). The red dotted line corresponds to the SIDM simulation with smooth star formation ($n_{\mathrm{th}} = 0.1\,\mathrm{cm}^{-3}$) and a self-interaction cross section $\sigma_T/m_\chi = 1\,\mathrm{cm}^2\mathrm{g}^{-1}$.

sion).

An adiabatic way to form a core is through elastic scattering between DM particles. Self-interacting DM (SIDM, [23–26]) redistributes energy outside-in, leading to the formation of a ~ 1 kpc size DM core in dwarf-size halos, provided the self-interaction cross section is $\sigma_T/m_\chi \sim 1\,\mathrm{cm}^2\mathrm{g}^{-1}$ on the scales of dwarf galaxies [24, 27, 28]. Such value of the cross section also evades current constraints [29–31], while for cross sections smaller by about an order of magnitude, SIDM is indistinguishable from CDM [32]. Contrary to SNF, SIDM causes the formation of cores in all haloes below a certain mass and, thus, observations of dwarf galaxies with cuspy host haloes (e.g. [31]) are more challenging to explain in SIDM (however, see [33] for a possible explanation).

In this *Letter* we use a suite of hydrodynamical simulations of an isolated dwarf galaxy to demonstrate that impulsive SNF produces distinct, shell-like kinematic signatures that appear in the phase space distribution of stars in dwarf galaxies – and argue that the systematic absence of such features across star-forming dwarf galaxies with confirmed cores, and in particular in dwarfs with recent starbursts, would point to an adiabatic core formation mechanism, such as SIDM.

II Simulations. The results presented here are derived from a suite of 16 high-resolution (with a DM particle mass $m_{\mathrm{DM}} \sim 1.3 \times 10^3 \mathrm{M}_\odot$ and a typical baryon mass $m_{\mathrm{b}} \sim 1.4 \times 10^3 \mathrm{M}_\odot$ [34] simulations of an isolated dwarf galaxy with a total baryonic mass of
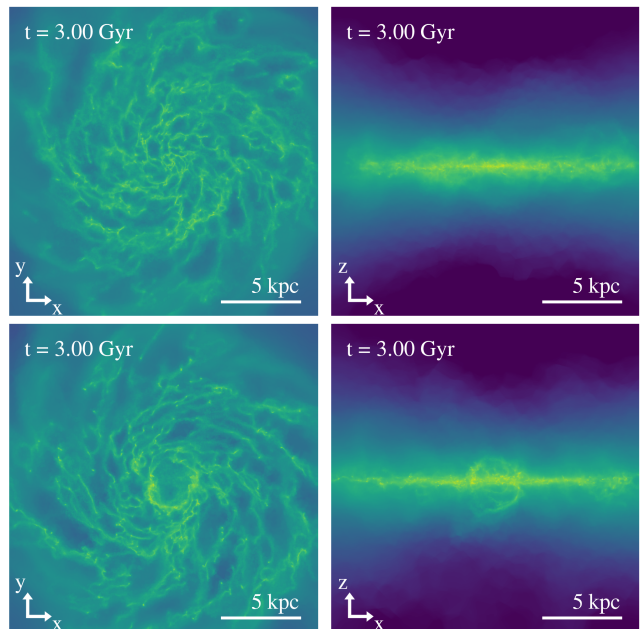

FIG. 2. Gas distributions of resulting galaxies after $3\,\mathrm{Gyr}$ of simulation time for two simulations with different star formation thresholds. We show face-on (left column) and edge-on (right column) projections of the gas density for the CDM simulation with smooth (top row) and bursty (bottom row) star formation. The side-length of the field of view is $20\,\mathrm{kpc}$ in each panel and we defined a coordinate system such that the z-axis is perpendicular to the gas disc. Notice how central gas is vertically expelled out of the disc plane in the simulation with bursty star formation. Such galactic outflows are characteristic of violent and impulsive events of supernova-driven energy release.

$M_b = 7.2 \times 10^8 \,\mathrm{M}_\odot$ and structural properties similar to those of the Small Magellanic Cloud (see [21, 22, 35],[36]). We use the formalism described in [37] to generate initial conditions of a system in approximate hydrostatic equilibrium. We then simulate the evolution of the isolated system, using the ISM model SMUGGLE [22] for the cosmological simulation code AREPO [38], along with the SIDM model presented in [24], for 16 different combinations of the star formation threshold n_{th} and the SIDM self-interaction cross section σ_T/m_χ. In Fig. 1, we demonstrate that nearly identical constant density DM cores can form adiabatically in SIDM simulations with smooth star formation histories (low values of n_{th}) and $\sigma_T/m_\chi \sim 1\,\mathrm{cm}^2\mathrm{g}^{-1}$ and through impulsive SNF in CDM simulations with bursty star formation histories (high values of n_{th}). While identical cores can form through SIDM and impulsive SNF, the phase space distribution of baryons is distinctly different between simulations with or without impulsive SNF, irrespective of whether DM is self-interacting. Hereafter, we illustrate this difference by comparing the results of the CDM runs with $n_{\mathrm{th}} = 0.1\,\mathrm{cm}^{-3}$ (representative of smooth SF and thus adiabatic SNF) and $n_{\mathrm{th}} = 100\,\mathrm{cm}^{-3}$ (representative of
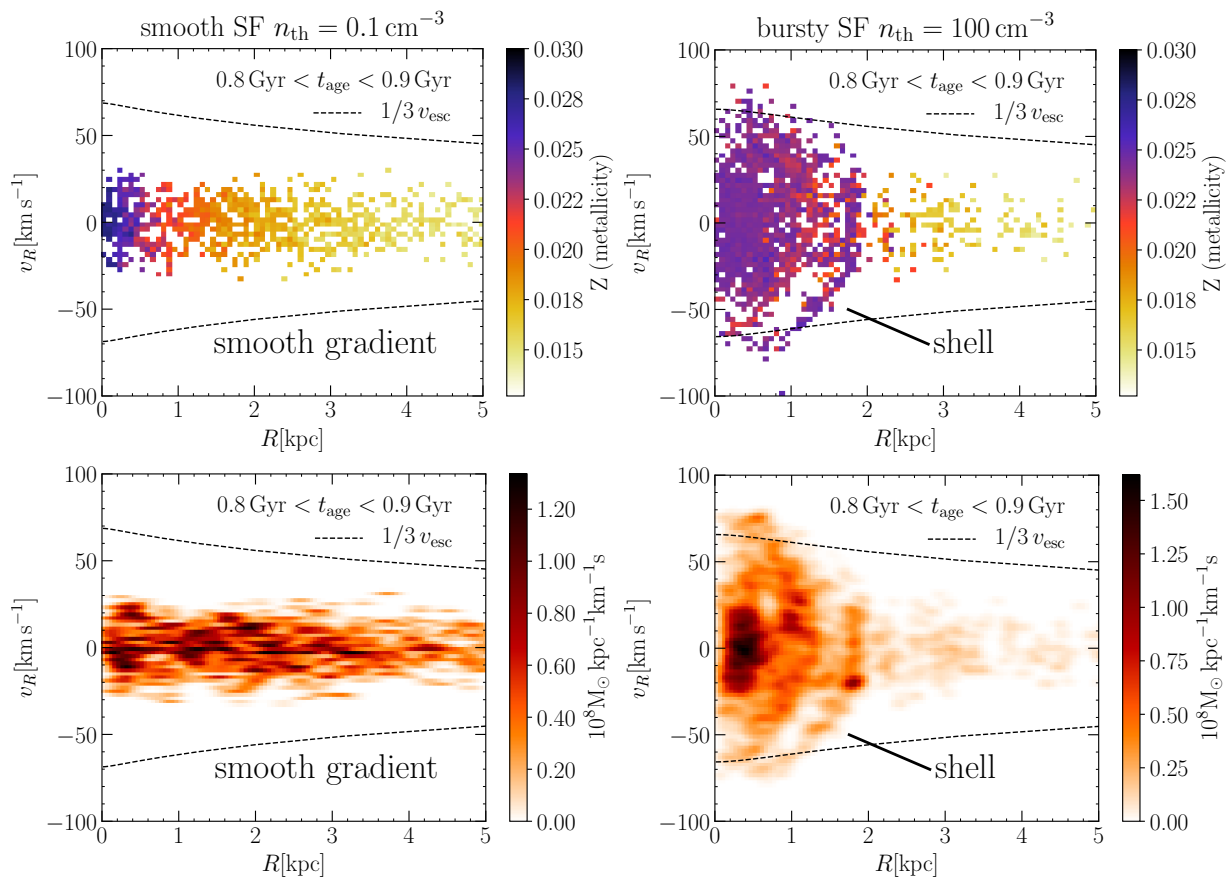
FIG. 3. Average metallicity distribution (top panels) and mass-weighted distribution function (bottom panels) of star particles calculated after $3\,\mathrm{Gyr}$ of simulation time for two different simulations, projected into the radial phase space ($R - v_R$). Star particles are subject to a cut in stellar age, only stars which are $0.8 - 0.9\,\mathrm{Gyr}$ old are shown in these plots. Averaged stellar metallicity (mass-weighted distribution function) is color-coded according to the scale on the right of each panel. For scale, we show a third of the escape velocity as a function of radius as black dashed lines. The left (right) column corresponds to the CDM simulation with smooth (bursty) star formation. Smooth star formation results in a smooth metallicity gradient with the enriched/younger starts in the centre. Bursty star formation results in an overall weaker gradient, along with the presence of a shell of stars with high metallicity that intersects a low metallicity population at $R \sim 2\,\mathrm{kpc}$. This shell appears as a distinct overdense region in the mass-weighted distribution function.

bursty SF and thus impulsive SNF).

Projections of the gas distribution after $3\,\mathrm{Gyr}$ of simulation time are shown in Fig. 2 for both benchmark simulations. The gas distributions of the two runs look strikingly different, in particular towards the centre of the galaxies. In the simulation with bursty SF – **and thus with impulsive SNF** – the central gas density is lower than in the immediate surroundings due to a supernova-driven gas outflow extending out of the galactic disc, which can be clearly appreciated as a nearly spherical bubble in the edge-on projection. In contrast, in the simulation with smooth SF, the edge-on projection of the gas appears rather regular and the face-on projection has no distinct features.

III Stellar phase space shells. Fig. 3 shows (for both benchmark CDM runs) the metallicity distribution and the mass-weighted distribution function of mono-age stars which are $0.8 - 0.9\,\mathrm{Gyr}$ old projected onto the $R - v_R$ plane at the end of the simulation. For the simulation

with smooth SF, we observe a steady decrease of the average metallicity of stars with increasing cylindrical radius, a natural consequence of the centrally concentrated star-forming gas. Statistically, more stars form in environments with higher gas densities, i.e., towards the centre of galaxies. Thus, the subsequent SNF cycles cause a metal enrichment of the ISM that is larger in the central regions. Therefore, stars of subsequent generations (like the ones shown in Fig. 3) acquire a negative metallicity gradient. Moreover, the radial velocities of stars are rather small in magnitude, $v_R \sim 25\,\mathrm{km\,s^{-1}}$ at most. A different picture emerges in the centre of the galaxy **with impulsive SNF**. Instead of a monotonic stellar metallicity gradient, a pattern of several shells in $R - v_R$ space emerges in the metallicity distribution – and the mass-weighted distribution function – of stars with similar ages. The shells are comprised of star particles with high metallicities, some of which move at radial speeds of more than $50\,\mathrm{km\,s^{-1}}$. These high metallicity shells

intersect phase space regions inhabited by more metal-poor star particles whose radial speeds are smaller on average. Such features are transient for a given group of stars, but occur at various times in the evolution, and are not unique to the CDM run with $n_{\rm th} = 100\,{\rm cm}^{-3}$; we find them also in other simulations (both in CDM and SIDM), **as long as the SF histories in these simulations are bursty – and SNF is impulsive. For our choice of initial conditions and fixed SMUGGLE parameters, the transition from smooth to bursty SF – and thus to impulsive SNF – happens around $n_{\rm th} = 10\,{\rm cm}^{-3}$ (see [16]). Notice that shells appear in all simulations in which SNF is impulsive – regardless of whether the DM is self-interacting or not.**

To quantify the difference between the final stellar distributions in the bursty SF case and in the smooth SF case **shown in Fig. 3**, we estimate the likelihood of randomly finding, in the smooth SF case, an overdensity similar to that associated with the clear shell in the bursty SF simulation. **We take the normalized, cumulative stellar mass distribution of the smooth SF simulation as a target distribution for random sampling and construct 10^7 re-sampled distributions, each time drawing as many radii as there are stars in the original distribution. For each re-sampled distribution, we then search a pre-defined "signal range" for the largest spherical overdensity that arises as a result of Poisson sampling [39]. We also calculate the overdensity at the position of the shell in the bursty SF simulation. From these values, we create a distribution of global (signal region) and local (shell area) overdensities. Comparison against the measured shell overdensity in the bursty SF simulation reveals that the shell has a global (local) significance of more than $5\,\sigma$ ($3.3\,\sigma$) compared to the smooth SF case.** These are conservative estimates for the significance of the shell-like feature since they are based on the stellar density distribution only and do not take into account information on the metallicity of stars. Finding an overdensity of such amplitude, combined with the observation that the overdensity consists mainly of high-metallicity stars, would be a smoking gun signature of an impulsive SNF cycle following an episode of bursty SF.

To determine how the shell-like features appear in the line-of-sight phase space of galaxies that are observed edge-on, we projected the distributions shown in Fig. 3 into $|x| - v_y$ space (**using the coordinate system defined in Fig. 2, [40]**). In the featureless smooth SF case, the emerging distribution of stars tracks the rotation curve of the galaxy, **with** a monotonic decrease of **(average)** metallicity with distance. In the bursty SF case, we observe two isolated overdense clusters consisting mainly of high metallicity stars, at a distance to the galaxy's centre of $\sim 2\,{\rm kpc}$, similar to the radius at which the phase space shell appears in Fig. 3. We explicitly confirmed that those clusters consist of the same stars as the

phase space shell. **We emphasize again that similar differences between the phase space distributions of stellar particles in galaxies with or without impulsive SNF emerge when SIDM simulations are considered.**

IV How shells are created. The shell-like features shown in Fig. 3 arise in the aftermath of starburst events – which are closely followed by impulsive episodes of SNF. **Reference [41] showed that young stars born in a turbulent ISM inherit the orbits of the star-forming gas and can be born with significant radial motion. The orbits of these stars are then further heated by subsequent feedback episodes, leading to sustained radial migration. The shells presented here form from such groups of stars, which are born during starburst events in a turbulent ISM. Such groups of stars constitute** *orbital families*[**16, 42**] **– sets of orbits defined by similar integrals of motion**[43]. **Moreover, they are born with similar metallicities and – as outlined above – with some initial amount of radial motion.**

Instead of causing a coherent net expansion, subsequent impulsive fluctuations in the gravitational potential discontinuously change the (gravitational) energy of a star (particle) by an amount that depends on its orbital phase [11, 42]. As a consequence, they can split an initially phase mixed *orbital family*, **i.e., create a distribution that is unmixed [16]. The phase space shells we observer are therefore signatures of the early stages of phase mixing [44, 45]. To compare this to the smooth case, we note that** in dynamical systems in which orbits are regular and stars act as dynamical tracers of the gravitational potential, the average metallicity of stars can only depend on their actions [46]. We can **therefore generally assume** *orbital families* **to be well approximated** by groups of stars with similar ages and metallicities. **Across our simulation suite,** we find that in simulations with impulsive SNF (following bursty SF), the energy distribution of *orbital families* is wider than in simulations with smooth SF [47], **a direct result of the period, SNF-driven heating of stellar orbits (see [42]).** The **shell-like signatures of** early-stage phase mixing observed here **are** thus a direct consequence of **impulsive SNF.**

V Discussion and outlook. **Finding stellar shells similar to the ones presented here in nearby dwarfs would imply a prior episode of impulsive SNF without necessarily establishing SNF as the dominant core formation mechanism.** In cosmological halos, we expect that diffusion caused by **the halo's triaxial shape** will erase the shells within ~ 1 dynamical time [42], implying that galaxies without recent bursty star formation (e.g. quenched galaxies) are fairly bad targets to look for phase space shells. Nevertheless, it is instructive to evaluate the potential of detecting such signatures of bursty SF in the Milky Way satellites, in particular Fornax [48–50], since it has been claimed to have

a core [5] (albeit this remains controversial, see [51]) and information on line-of-sight kinematics, metallicity [48], and age [49] is available for a sub-sample of its member stars. Unfortunately, we find that the ages of individual stars carry uncertainties which are too large (~ 1 Gyr) to conclusively **identify** *orbital families*. Ideal future targets to look for impulsive SNF signatures are star-forming field dwarfs in the vicinity of the Local Group **(see [4])**. **At the current time, the number of resolved stars with known ages and metallicities in these galaxies is too small.** Within the next decade, **however**, the Roman Space Telescope will provide precise photometric data of individual stars in dwarf galaxies within the Local Volume [52]. Combined with spectroscopic data from the ground, this will enable the precision needed to determine the ages, metallicities, and kinematics of a sufficient number of stars to conclusively establish whether the characteristic shell-like signatures of impulsive SNF presented here **– or rather their projections into the space of line-of-sight velocity vs projected radius [53] –** are ubiquitously present or **systematically** absent. **Further in the future, new generations of extremely large telescopes (ELTs) may even provide sufficiently precise data on the 3d motions of stars in nearby dwarfs to allow for a search of shells directly in $R - v_R$ space [54].**

The significance of a (potential) non-detection of such shells in dwarf galaxies with a core also depends on how robust our results are to changes in the initial setup or the stellar evolution model. Apart from the host halo's triaxiality, two effects that we do not explicitly test for may be significant. First, SF histories in real dwarf galaxies may be bursty, but starbursts may occur away from the galaxy's center. However, SNF needs to impulsively change the central potential to be a feasible core formation mechanism (see [11, 16]). The non-detection of kinematic signatures would then require starbursts to occur mainly in the center of dwarfs, but exclusively off-center at late times; a possible but unlikely scenario (see [41]). Second, stellar clusters (i.e. *orbital families*) born in starburst events need to contain a sufficient

number of stars to allow us to identify shells formed from them. Based on our re-sampling routine [55], we estimate that a shell needs to contain a few hundred stars to be significant at a 2σ level (notice that this implies that future experiments need to provide precise age and metallicity information for $\mathcal{O}(10^4)$ stars if we assume a constant average SF rate). In a detailed high-resolution study of the impact of different kinds of stellar feedback, [56] found that clusters of such size formed in all simulations in which SNF was included. At this time, we are unaware of any study in which no clusters of at least ~ 100 stars form, while SNF is modeled self-consistently and found it to be a feasible core formation mechanism.

We thus infer that the conclusive, systematic absence of signatures of impulsive SNF **across all** isolated, star-forming field dwarfs with confirmed cores would give strong support to alternative DM models, such as SIDM.

ACKNOWLEDGMENTS

[1] J. S. Bullock and M. Boylan-Kolchin, Small-Scale Challenges to the ΛCDM Paradigm, Annual Review of Astron and Astrophys **55**, 343 (2017), arXiv:1707.04256.

[2] B. Moore, Evidence against dissipation-less dark matter from observations of galaxy haloes, Nature **370**, 629 (1994).

[3] R. Kuzio de Naray, S. S. McGaugh, and W. J. G. de Blok, Mass Models for Low Surface Brightness Galaxies with High-Resolution Optical Velocity Fields, Astrophysical Journal **676**, 920 (2008), arXiv:0712.0860.

[4] J. I. Read, M. G. Walker, and P. Steger, Dark matter heats up in dwarf galaxies, Monthly Notices of the RAS **484**, 1401 (2019), arXiv:1808.06634 [astro-ph.GA].

[5] M. G. Walker and J. Peñarrubia, A Method for Measuring (Slopes of) the Mass Profiles of Dwarf Spheroidal Galaxies, Astrophysical Journal **742**, 20 (2011), arXiv:1108.2404 [astro-ph.CO].

[6] S.-H. Oh, W. J. G. de Blok, E. Brinks, F. Walter, and J. Kennicutt, Robert C., Dark and Luminous Matter in THINGS Dwarf Galaxies, Astronomical Journal **141**, 193 (2011), arXiv:1011.0899 [astro-ph.CO].

[7] S.-H. Oh, D. A. Hunter, E. Brinks, B. G. Elmegreen, A. Schruba, F. Walter, M. P. Rupen, L. M. Young, C. E. Simpson, M. C. Johnson, K. A. Herrmann, D. Ficut-

Vicas, P. Cigan, V. Heesen, T. Ashley, and H.-X. Zhang, High-resolution Mass Models of Dwarf Galaxies from LITTLE THINGS, Astronomical Journal **149**, 180 (2015), arXiv:1502.01281 [astro-ph.GA].

[8] J. F. Navarro, C. S. Frenk, and S. D. M. White, The Structure of Cold Dark Matter Halos, Astrophysical Journal **462**, 563 (1996), arXiv:astro-ph/9508025 [astro-ph].

[9] J. Wang, S. Bose, C. S. Frenk, L. Gao, A. Jenkins, V. Springel, and S. D. M. White, Universal structure of dark matter haloes over a mass range of 20 orders of magnitude, Nature **585**, 39 (2020), arXiv:1911.09720 [astro-ph.CO].

[10] J. F. Navarro, V. R. Eke, and C. S. Frenk, The cores of dwarf galaxy haloes, Monthly Notices of the RAS **283**, L72 (1996), astro-ph/9610187.

[11] A. Pontzen and F. Governato, How supernova feedback turns dark matter cusps into cores, Monthly Notices of the RAS **421**, 3464 (2012), arXiv:1106.0499 [astro-ph.CO].

[12] A. Di Cintio, C. B. Brook, A. V. Macciò, G. S. Stinson, A. Knebe, A. A. Dutton, and J. Wadsley, The dependence of dark matter profiles on the stellar-to-halo mass ratio: a prediction for cusps versus cores, Monthly Notices of the RAS **437**, 415 (2014), arXiv:1306.0898.

[13] A. Benítez-Llambay, C. S. Frenk, A. D. Ludlow, and J. F. Navarro, Baryon-induced dark matter cores in the EAGLE simulations, Monthly Notices of the RAS **488**, 2387 (2019), arXiv:1810.04186 [astro-ph.GA].

[14] A. Lazar, J. S. Bullock, M. Boylan-Kolchin, T. K. Chan, P. F. Hopkins, A. S. Graus, A. Wetzel, K. El-Badry, C. Wheeler, M. C. Straight, D. Kereš, C.-A. Faucher-Giguère, A. Fitts, and S. Garrison-Kimmel, A dark matter profile to model diverse feedback-induced core sizes of ΛCDM haloes, Monthly Notices of the RAS **497**, 2393 (2020), arXiv:2004.10817 [astro-ph.GA].

[15] A. A. Dutton, T. Buck, A. V. Macciò, K. L. Dixon, M. Blank, and A. Obreja, NIHAO - XXV. Convergence in the cusp-core transformation of cold dark matter haloes at high star formation thresholds, Monthly Notices of the RAS **499**, 2648 (2020), arXiv:2011.11351 [astro-ph.GA].

[16] J. D. Burger and J. Zavala, Supernova-driven Mechanism of Cusp-core Transformation: an Appraisal, ApJ **921**, 126 (2021), arXiv:2103.01231 [astro-ph.GA].

[17] S. Bose, C. S. Frenk, A. Jenkins, A. Fattahi, F. A. Gómez, R. J. J. Grand, F. Marinacci, J. F. Navarro, K. A. Oman, R. Pakmor, J. Schaye, C. M. Simpson, and V. Springel, No cores in dark matter-dominated dwarf galaxies with bursty star formation histories, MNRAS **486**, 4790 (2019), arXiv:1810.03635 [astro-ph.GA].

[18] G. Kauffmann, Quantitative constraints on starburst cycles in galaxies with stellar masses in the range 10^8-10^{10} M$_\odot$, Monthly Notices of the RAS **441**, 2717 (2014).

[19] D. R. Weisz, A. E. Dolphin, E. D. Skillman, J. Holtzman, K. M. Gilbert, J. J. Dalcanton, and B. F. Williams, The Star Formation Histories of Local Group Dwarf Galaxies. I. Hubble Space Telescope/Wide Field Planetary Camera 2 Observations, Astrophysical Journal **789**, 147 (2014), arXiv:1404.7144.

[20] N. Emami, B. Siana, D. R. Weisz, B. D. Johnson, X. Ma, and K. El-Badry, A Closer Look at Bursty Star Formation with L$_{H\alpha}$ and L$_{UV}$ Distributions, Astrophysical Journal **881**, 71 (2019), arXiv:1809.06380 [astro-ph.GA].

[21] P. F. Hopkins, E. Quataert, and N. Murray, The struc-ture of the interstellar medium of star-forming galaxies, Monthly Notices of the RAS **421**, 3488 (2012), arXiv:1110.4636 [astro-ph.CO].

[22] F. Marinacci, L. V. Sales, M. Vogelsberger, P. Torrey, and V. Springel, Simulating the interstellar medium and stellar feedback on a moving mesh: implementation and isolated galaxies, Monthly Notices of the RAS **489**, 4233 (2019), arXiv:1905.08806 [astro-ph.GA].

[23] D. N. Spergel and P. J. Steinhardt, Observational Evidence for Self-Interacting Cold Dark Matter, Physical Review Letters **84**, 3760 (2000), astro-ph/9909386.

[24] M. Vogelsberger, J. Zavala, and A. Loeb, Subhaloes in self-interacting galactic dark matter haloes, Monthly Notices of the RAS **423**, 3740 (2012), arXiv:1201.5892.

[25] M. Rocha, A. H. G. Peter, J. S. Bullock, M. Kaplinghat, S. Garrison-Kimmel, J. Oñorbe, and L. A. Moustakas, Cosmological simulations with self-interacting dark matter - I. Constant-density cores and substructure, Monthly Notices of the RAS **430**, 81 (2013), arXiv:1208.3025.

[26] S. Tulin and H.-B. Yu, Dark matter self-interactions and small scale structure, Physics Reports **730**, 1 (2018), arXiv:1705.02358 [hep-ph].

[27] A. H. G. Peter, M. Rocha, J. S. Bullock, and M. Kaplinghat, Cosmological simulations with self-interacting dark matter - II. Halo shapes versus observations, Monthly Notices of the RAS **430**, 105 (2013), arXiv:1208.3026.

[28] M. Kaplinghat, S. Tulin, and H.-B. Yu, Dark Matter Halos as Particle Colliders: Unified Solution to Small-Scale Structure Puzzles from Dwarfs to Clusters, Physical Review Letters **116**, 041302 (2016), arXiv:1508.03339 [astro-ph.CO].

[29] A. Robertson, R. Massey, and V. Eke, What does the Bullet Cluster tell us about self-interacting dark matter?, Monthly Notices of the RAS **465**, 569 (2017), arXiv:1605.04307.

[30] A. Robertson, D. Harvey, R. Massey, V. Eke, I. G. McCarthy, M. Jauzac, B. Li, and J. Schaye, Observable tests of self-interacting dark matter in galaxy clusters: cosmological simulations with SIDM and baryons, ArXiv e-prints (2018), arXiv:1810.05649.

[31] J. I. Read, M. G. Walker, and P. Steger, The case for a cold dark matter cusp in Draco, Monthly Notices of the RAS **481**, 860 (2018), arXiv:1805.06934.

[32] J. Zavala, M. Vogelsberger, and M. G. Walker, Constraining self-interacting dark matter with the Milky Way's dwarf spheroidals, Monthly Notices of the RAS **431**, L20 (2013), arXiv:1211.6426 [astro-ph.CO].

[33] J. Zavala, M. R. Lovell, M. Vogelsberger, and J. D. Burger, Diverse dark matter density at sub-kiloparsec scales in Milky Way satellites: Implications for the nature of dark matter, Physical Review D **100**, 063007 (2019), arXiv:1904.09998 [astro-ph.GA].

[34] See Section IA of the Supplemental Material – which contains additional references [57–61] – for a discussion of how the initial conditions are generated.

[35] J. D. Burger, J. Zavala, L. V. Sales, M. Vogelsberger, F. Marinacci, and P. Torrey, Degeneracies between self-interacting dark matter and supernova feedback as cusp-core transformation mechanisms, MNRAS **513**, 3458 (2022), arXiv:2108.07358 [astro-ph.GA].

[36] See also Section IB of the Supplemental Material – which contains additional references [62–68] – for further details on the simulation suite.

[37] V. Springel and L. Hernquist, Cosmological smoothed

particle hydrodynamics simulations: a hybrid multiphase model for star formation, Monthly Notices of the RAS **339**, 289 (2003), arXiv:astro-ph/0206393 [astro-ph].

[38] V. Springel, E pur si muove: Galiliean-invariant cosmological hydrodynamical simulations on a moving mesh, Monthly Notices of the RAS **401**, 791 (2010), arXiv:0901.4107 [astro-ph.CO].

[39] See Section ID of the Supplemental Material for a more detailed description of the resampling procedure.

[40] See Supplemental Fig. 3. See also Section IC of the Supplemental Material for a descriptions of how the simulated data are processed to produce the results presented here.

[41] K. El-Badry, A. Wetzel, M. Geha, P. F. Hopkins, D. Kereš, T. K. Chan, and C.-A. Faucher-Giguère, Breathing FIRE: How Stellar Feedback Drives Radial Migration, Rapid Size Fluctuations, and Population Gradients in Low-mass Galaxies, Astrophys. J. **820**, 131 (2016), arXiv:1512.01235 [astro-ph.GA].

[42] J. D. Burger and J. Zavala, The nature of core formation in dark matter haloes: adiabatic or impulsive?, Monthly Notices of the RAS **485**, 1008 (2019), arXiv:1810.10024 [astro-ph.GA].

[43] See also Section II of the Supplemental Material for a closer look at the shell formation mechanism.

[44] J. Binney and S. Tremaine, *Galactic Dynamics: Second Edition* (2008).

[45] W. Dehnen and J. I. Read, N-body simulations of gravitational dynamics, European Physical Journal Plus **126**, 55 (2011), arXiv:1105.1082 [astro-ph.IM].

[46] A. M. Price-Whelan, D. W. Hogg, K. V. Johnston, M. K. Ness, H.-W. Rix, R. L. Beaton, J. R. Brownstein, D. A. García-Hernández, S. Hasselquist, C. R. Hayes, R. R. Lane, M. Shetrone, J. Sobeck, and G. Zasowski, Orbital Torus Imaging: Using Element Abundances to Map Orbits and Mass in the Milky Way, Astrophysical Journal **910**, 17 (2021), arXiv:2012.00015 [astro-ph.GA].

[47] See also Section IC of the Supplemental Material, in particular Supplemental Fig. 5.

[48] M. G. Walker, M. Mateo, and E. W. Olszewski, Stellar Velocities in the Carina, Fornax, Sculptor, and Sextans dSph Galaxies: Data From the Magellan/MMFS Survey, Astronomical Journal **137**, 3100 (2009), arXiv:0811.0118 [astro-ph].

[49] T. J. L. de Boer, E. Tolstoy, V. Hill, A. Saha, E. W. Olszewski, M. Mateo, E. Starkenburg, G. Battaglia, and M. G. Walker, The star formation and chemical evolution history of the Fornax dwarf spheroidal galaxy, Astronomy & Astrophysics **544**, A73 (2012), arXiv:1206.6968 [astro-ph.GA].

[50] V. Rusakov, M. Monelli, C. Gallart, T. K. Fritz, T. Ruiz-Lara, E. J. Bernard, and S. Cassisi, The bursty star formation history of the Fornax dwarf spheroidal galaxy revealed with the HST, Monthly Notices of the RAS **502**, 642 (2021), arXiv:2002.09714 [astro-ph.GA].

[51] A. Genina, A. Benítez-Llambay, C. S. Frenk, S. Cole, A. Fattahi, J. F. Navarro, K. A. Oman, T. Sawala, and T. Theuns, The core-cusp problem: a matter of perspective, Monthly Notices of the RAS **474**, 1398 (2018), arXiv:1707.06303 [astro-ph.GA].

[52] R. Khan, B. F. Williams, J. Dalcanton, and WFIRST Infrared Nearby Galaxies Survey (WINGS), WFIRST: Simulating and Analyzing Wide Field, High-Resolution Images of Nearby Galaxies, in *American Astronomical Society Meeting Abstracts #231*, American Astronomical Society Meeting Abstracts, Vol. 231 (2018) p. 150.40.

[53] See Supplemental Fig. 3.

[54] J. Simon, S. Birrer, K. Bechtol, S. Chakrabarti, F.-Y. Cyr-Racine, I. Dell'Antonio, A. Drlica-Wagner, C. Fassnacht, M. Geha, D. Gilman, Y. D. Hezaveh, D. Kim, T. S. Li, L. Strigari, and T. Treu, Testing the Nature of Dark Matter with Extremely Large Telescopes, BAAS **51**, 153 (2019), arXiv:1903.04742 [astro-ph.CO].

[55] See Section ID of the Supplemental Material.

[56] M. C. Smith, G. L. Bryan, R. S. Somerville, C.-Y. Hu, R. Teyssier, B. Burkhart, and L. Hernquist, Efficient early stellar feedback can suppress galactic outflows by reducing supernova clustering, MNRAS **506**, 3882 (2021), arXiv:2009.11309 [astro-ph.GA].

[57] L. Hernquist, An Analytical Model for Spherical Galaxies and Bulges, Astrophys. J. **356**, 359 (1990).

[58] V. Springel, T. Di Matteo, and L. Hernquist, Modelling feedback from stars and black holes in galaxy mergers, Monthly Notices of the RAS **361**, 776 (2005), arXiv:astro-ph/0411108 [astro-ph].

[59] M. Asplund, N. Grevesse, A. J. Sauval, and P. Scott, The Chemical Composition of the Sun, Annual Review of Astronomy and Astrophysics **47**, 481 (2009), arXiv:0909.0948 [astro-ph.SR].

[60] A. S. Eddington, The distribution of stars in globular clusters, Monthly Notices of the RAS **76**, 572 (1916).

[61] L. Hernquist, N-Body Realizations of Compound Galaxies, Astrophysical Journal Supplement **86**, 389 (1993).

[62] M. R. Krumholz and J. C. Tan, Slow Star Formation in Dense Gas: Evidence and Implications, Astrophysical Journal **654**, 304 (2007), arXiv:astro-ph/0606277 [astro-ph].

[63] S. Balberg, S. L. Shapiro, and S. Inagaki, Self-Interacting Dark Matter Halos and the Gravothermal Catastrophe, Astrophysical Journal **568**, 475 (2002), arXiv:astro-ph/0110561 [astro-ph].

[64] P. Colín, V. Avila-Reese, O. Valenzuela, and C. Firmani, Structure and Subhalo Population of Halos in a Self-interacting Dark Matter Cosmology, Astrophysical Journal **581**, 777 (2002), arXiv:astro-ph/0205322 [astro-ph].

[65] J. Koda and P. R. Shapiro, Gravothermal collapse of isolated self-interacting dark matter haloes: N-body simulation versus the fluid model, Monthly Notices of the RAS **415**, 1125 (2011), arXiv:1101.3097 [astro-ph.CO].

[66] J. Pollack, D. N. Spergel, and P. J. Steinhardt, Supermassive Black Holes from Ultra-strongly Self-interacting Dark Matter, Astrophysical Journal **804**, 131 (2015), arXiv:1501.00017 [astro-ph.CO].

[67] H. Nishikawa, K. K. Boddy, and M. Kaplinghat, Accelerated core collapse in tidally stripped self-interacting dark matter halos, Physical Review D **101**, 063009 (2020), arXiv:1901.00499 [astro-ph.GA].

[68] C. Power, J. F. Navarro, A. Jenkins, C. S. Frenk, S. D. M. White, V. Springel, J. Stadel, and T. R. Quinn, The Inner structure of Lambda CDM halos. 1. A Numerical convergence study, Monthly Notices of the RAS **338**, 14 (2003), arXiv:astro-ph/0201544 [astro-ph].